

Half-metallic ferromagnetism character induced by V-doped cubic AlN

Miguel J. Espitia R.¹, John H. Díaz F.¹, Octavio José Salcedo Parra^{2,3}

¹GEFEM Group, Universidad Distrital “Francisco José de Caldas”, Bogotá, Colombia.

²Internet Inteligente Research Group, Universidad Distrital “Francisco José de Caldas”, Bogotá, Colombia.

³Faculty of Engineering - Universidad Nacional de Colombia, Bogotá D.C., Colombia.

Abstract

Computational calculations were performed for study the structural, electronic, and magnetic properties of the $\text{Al}_{0.0625}\text{V}_{0.9375}\text{N}$, and $\text{Al}_{0.125}\text{V}_{0.875}\text{N}$ compounds in the cubic zincblende phase, using density functional theory. The calculations were carried out by means of the pseudopotential method, employing computational Quantum ESPRESSO code. The density of states show that the compounds have a half-metallic character. The calculated total magnetic moments of $\text{Al}_{0.0625}\text{V}_{0.9375}\text{N}$, and $\text{Al}_{0.125}\text{V}_{0.875}\text{N}$ were $2.0 \mu_B$ and $4.0 \mu_B$ per cell, respectively, the mainly being contribution to the total magnetic moment the 3d-V orbital. The computational calculations predict a Curie temperature of $\sim 410.8 \text{ }^\circ\text{K}$, which is higher than room temperature. The results suggest that, AlN doped with V is a promising candidate to be a good diluted magnetic semiconductor material.

Keywords: Half-metallic ferromagnetism, diluted magnetic semiconductor, electronic and magnetic properties.

INTRODUCCIÓN

The aluminum nitride (AlN) is semiconductor material, has been studied theoretical and experimentally. The AlN have high thermal stability, high melting point, high thermal conductivity, large bulk modulus, high chemical stability, very strong bond strength, and low compressibility. Due to these properties, along with its large band-gap energy, AlN has potential technological applications for high-temperature transistors, light-emitting diodes (LEDs) in the violet, blue, and green regions, lasers, and optical detectors [1, 2, 3]. Actually, AlN is widely used in the semiconductor industry, and many of its potential applications are a reality. Some electronic and optoelectronic devices are now available commercially [4], such as green [5] and blue [6] LEDs and lasers [7]. Additionally, in recent years several theoretical investigations [8–17] and experimental studies [18–27] have found that AlN doped with transition metals (TM) [28–30] turned out to be a good diluted magnetic semiconductor for use in spintronics devices. All these studies of TM-doped AlN were made in the wurtzite structure, because the wurtzite phase is the ground state of AlN. however, recently there has been a lot of interest in AlN in the zincblende structure, because AlN-zincblende has been grown by different experimental techniques, such as solid-state reaction [31], molecular beam epitaxy MBE [4], the

vapor–liquid–solid (VLS) route [32], and reactive pulsed laser deposition [33]. Though it is expected that AlN zincblende applications will be similar to those developed for AlN wurtzite, many researchers have found several advantages of the zincblende over the wurtzite structure [34–36], because the zincblende phase of AlN doesn't have a polarized internal electric field [37], due to its high crystallographic symmetry. The absence of an internal electric field in AlN zincblende improves its electronic properties, because of higher carrier mobility, higher drift velocities, and better doping efficiencies [34–36]. At the same time, there are additional advantages for group-III semiconductors in the cubic phase; for example, in GaN zincblende it was found that there is a reduction in the radiative recombination time by two orders of magnitude compared to GaN wurtzite [38]. In spite of cubic AlN have better performance and the technological developments for the growth of AlN in zincblende structure are now available, very few theoretical researches have been made for zincblende AlN doped with V [39]. In this paper, we focus our study in the structural, electronic, and magnetic properties of AlN zincblende doped with vanadium in the concentrations of $\text{Al}_{0.0625}\text{V}_{0.9375}\text{N}$, and $\text{Al}_{0.125}\text{V}_{0.875}\text{N}$, due to possible use as diluted magnetic semiconductor material.

COMPUTATIONAL METHOD

We performed calculations using the Quantum ESPRESSO computational code [40] based in the pseudopotential method [41, 42] within density functional theory (DFT) [43, 44]. The correlation and exchange effects between electrons were taken into account with the generalized gradient approximation (GGA) of Perdew, Burke, and Ernzerhof (PBE) [45]. For the expansion of the electronic function in plane waves, we used values of kinetic energy cutoff and charge density of 40 Ry and 400 Ry, respectively. Brillouin zone integrations were performed with the special k-point method over a $6 \times 6 \times 12$ Monkhorst-Pack mesh [46] for a unit cell. To simulate pristine AlN in the zincblende structure, we constructed a $2a \times 2b \times 1c$ supercell with 32 atoms (fig. 1). For the concentration $\text{Al}_{0.0625}\text{V}_{0.9375}\text{N}$, and $\text{Al}_{0.125}\text{V}_{0.875}\text{N}$ one and two Al atoms were replaced by one and two V atoms respectively, in the supercell. For the pure AlN compound and $\text{Al}_{0.0625}\text{V}_{0.9375}\text{N}$, and $\text{Al}_{0.125}\text{V}_{0.875}\text{N}$ concentrations, were performed a vc-relax type calculation in which all atoms in the supercell move in the three directions and the same time the lattice constants the supercell

are varying. All calculations were carried out with spin polarization, and the optimization process ended when the forces became smaller than 10^{-4} eV/Å. The convergence threshold for self-consistent field iteration was 10^{-5} eV.

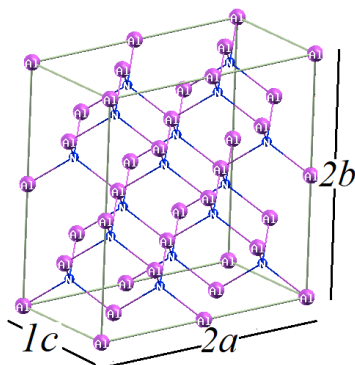


Figure 1. Conventional unit cell of pure AlN in the zincblende structure. Source: Authors

RESULTS AND DISCUSSIONS

Structural properties

To evaluate the equilibrium parameters, such as the lattice constant (a_0), bulk modulus (B_0), and total energy (E_0) of pristine AlN, $\text{Al}_{0.0625}\text{V}_{0.9375}\text{N}$, and $\text{Al}_{0.125}\text{V}_{0.875}\text{N}$ in the zincblende phase, we carried out a minimization process of the total energy using vc-relax calculations. All calculations were carry out with spin-polarized. Additionally, in order to establish the magnetic phase most stable for the $\text{Al}_{0.125}\text{V}_{0.875}\text{N}$ compound the ferromagnetic (FM) and antiferromagnetic (AFM) phases were calculated, several AFM configurations with different spin orientations were considered until obtaining the most stable structure.

Table 1: Lattice constant, bulk modulus, total energy of $\text{Al}_{0.0625}\text{V}_{0.9375}\text{N}$, and $\text{Al}_{0.125}\text{V}_{0.875}\text{N}$ in the zincblende structure.

Compound	a (Å)	B_0 (GPa)	E_0 (eV)
Pristine-AlN	4.3815	206.52	
	4.3800 ^a	212.70 ^b	
	4.3790 ^c	211.78 ^d	- 7101.0310
	4.3700 ^e	202.00 ^e	
$\text{Al}_{0.0625}\text{V}_{0.9375}\text{N}$	4.3710	196.83	- 8884.4126
FM- $\text{Al}_{0.125}\text{V}_{0.875}\text{N}$	4.3682	189.85	-10668.1608
AFM- $\text{Al}_{0.125}\text{V}_{0.875}\text{N}$	4.3698	189.98	-10668.1254

^aTheoretical Reference [47].

^bTheoretical Reference [48].

^cTheoretical Reference [49].

^dTheoretical Reference [50].

^e Experimental Reference [51].

In the table 1 are listed the resulting the equilibrium lattice constant, bulk modulus and total minimum energy along with experimental and theoretical recent reported. We obtained for the lattice constant 4.3815 Å for AlN-zincblende, in comparison with the experimental value 4.3700 Å [51], the error in lattice constant was $\sim 0.263\%$, while the maximum discrepancy with value reported theoretically. 4.3790 Å [49] was $\sim 0.13\%$. In both cases, the difference is less than 1%. Therefore, the calculated lattice constant pure AlN-zincblende is in very good agreement with reported experimental and theoretically values. For the calculated value of the bulk modulus, 206.52 GPa the error in comparison with experimental value 202.00 GPa [51] was $\sim 2.23\%$. We observed that the value of the calculated bulk modulus here is closer to the experimental value than those reported by other authors; hence the values reported for the lattice constant and the bulk modulus are acceptable.

We note that in the $\text{Al}_{0.0625}\text{V}_{0.9375}\text{N}$, and $\text{Al}_{0.125}\text{V}_{0.875}\text{N}$ compounds, the equilibrium lattice constant diminishes slightly with respect to pure AlN-zincblende compound. This occur because the radius of the V atom (1.34 Å) is smaller than the atomic radius of Al (1.43 Å).

According to the values of the total energy for the $\text{Al}_{0.125}\text{V}_{0.875}\text{N}$ compound in Table 1, the FM phase is smaller than the AFM one. The energy difference between the FM and the AFM phases is defined as $\Delta E = E_{AFM} - E_{FM}$, about 354 meV. Therefore, the ground state of V-doped AlN-zincblende is ferromagnetic.

In order to check the relative stability for $\text{Al}_{0.0625}\text{V}_{0.9375}\text{N}$, and $\text{Al}_{0.125}\text{V}_{0.875}\text{N}$ in the zincblende structure, we estimated the formation energy for each concentration, the formation energy is definite as [30]:

$$E_f = E_{V:AIN} - E_{AIN} - mE_V + mE_{Al}$$

Where, $E_{V:AIN}$, E_{AIN} , E_V and E_{Al} are the total energies of V-doped AlN, pristine AlN zincblende, cubic center body bcc-V and cubic center face fcc-Al. m is the number of V atoms that occupy the positions of the Al atoms. The calculated values of the formation energy for a single o pair V doped AlN zincblende, namely, $\text{Al}_{0.0625}\text{V}_{0.9375}\text{N}$, and $\text{Al}_{0.125}\text{V}_{0.875}\text{N}$ concentration were: 2.712 eV and 5.058 eV, respectively. When comparing the formation energy for the formation energy in the zincblende structure calculated here with the formation energy in the wurtzite structure of 2.49 eV and 4.91 [52], we observe that they are close. This, as well as the moderate values for formation energy of $\text{Al}_{0.0625}\text{V}_{0.9375}\text{N}$, and $\text{Al}_{0.125}\text{V}_{0.875}\text{N}$ compounds indicate that can be easily grown.

Electronic Properties

The band structure and spin-polarized density of states (DOS) along the symmetry path of pristine AlN, $\text{Al}_{0.0625}\text{V}_{0.9375}\text{N}$, and $\text{Al}_{0.125}\text{V}_{0.875}\text{N}$ in the zincblende structure were calculated with the equilibrium lattice constant show in table 1. The band structure and DOS are shown in the fig. 2, and fig. 3, respectively. Where we have chosen the Fermi Level as zero of energy.

In Fig. 2(a), we can see that pristine AlN-zincblende is an indirect band gap semiconductor material, with the top of the valence band located at the X point and the bottom of the conduction band located at the Γ point of the Brillouin zone. The calculated value of energy band is 3.37 eV, which is very close to previous theoretical results 3.38 eV [53], 3.40 eV [54] and 3.36 eV [55].

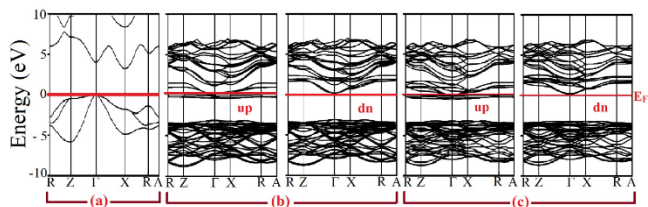


Figure 2. Band structure in the zincblende phase of (a) pristine AlN, (b) $\text{AlC}_{0.0625}\text{N}_{0.9375}$, and (c) $\text{AlC}_{0.125}\text{N}_{0.875}$. Source: Authors.

Fig. 2(a)-(b) shows the spin up and spin down band structure of the $\text{Al}_{0.0625}\text{V}_{0.9375}\text{N}$ and $\text{Al}_{0.125}\text{V}_{0.875}\text{N}$ concentrations. The band structure exhibits a half-metallic character, with the spin down being semiconducting and the spin up being metallic. Above the Fermi level, the band structure exhibits a dispersed band. Due to the spin up orientation's being partially filled, there are enough states behaving like free holes. Consequently, these compounds have 100% spin polarization of the conduction carriers and satisfy this requirement for use as spin injectors [56-58].

In the fig. 3(a) and fig. 3 (b) it is observed the DOS of $\text{Al}_{0.0625}\text{V}_{0.9375}\text{N}$, and $\text{Al}_{0.125}\text{V}_{0.875}\text{N}$, when one and two V atoms occupy the positions of the Al atoms. With the DOS, it is verified once more that the compounds exhibit a half-metallic character, because only the spin channel (spin up) crosses the Fermi level. The DOS of the $\text{Al}_{0.0625}\text{V}_{0.9375}\text{N}$ and $\text{Al}_{0.125}\text{V}_{0.875}\text{N}$ compounds shows that the spin density is mainly situated around the V atom, with a minimum contribution of the first-neighbor N atoms. For this reason, near the Fermi Level the mainly contribution to total DOS comes from of 3d-V orbital with minor contribution of 2p-N orbital. The hybridization and polarization between 3d-V and 2p-N generate a magnetic moment finite in $\text{Al}_{0.0625}\text{V}_{0.9375}\text{N}$, and $\text{Al}_{0.125}\text{V}_{0.875}\text{N}$ compounds, with values of $2.0 \mu_B$ and $4.0 \mu_B$ per cell. The values of magnetic moment are integers, this confirm that the half-metallic ferromagnetic character of the compounds. The mechanism by means of which the half-metallic ferromagnetic state is stabilized in V-doped AlN in the zincblende structure can be explained as follows: When an Al atom is replaced with a V atom in the zincblende structure, four N atoms surround the vanadium atom, thereby the V atom is located in a tetrahedral symmetry generated by the N atoms, as shown in Fig. 4(a). Additionally, the crystal field theory ensures that, the tetrahedral symmetry splits the five energy levels of the 3d orbital into three-fold high-energy degenerate states (d_{xy} , d_{xz} and, d_{yz}) called t_{2g} and two-fold low-energy degenerate state (d_{z^2} and $d_{x^2-y^2}$) denominated e_g [59]. At this point, it is pertinent to remember that the V atom has three valence

electrons located in the 3d-orbital. Therefore, two occupy the doubly-degenerate state e_g and one occupies the triply degenerate state t_{2g} . The low-energy e_g state is fully occupied, while the high-energy t_{2g} state is partially filled (just 1/3). Due of this the Fermi energy is located in the lower part of the t_{2g} state and leaves two electronic states per V atom empty (as shown Fig. 4(b), in which we can see the split between e_g and t_{2g} due to tetrahedral symmetry for both up-spin and down-spin, but not shown are electrons located in the e_g or t_{2g} states of the down-spin, because in accordance with the density of state, Fig. 3, close to the Fermi level there is no contribution from the down-spin). Hence, the fact that the high-energy t_{2g} state is partially filled indicates that the ferromagnetic ground state is associated with a split due to a symmetric tetrahedral, and with the double-exchange mechanism (which was well explained by Dietl et al. [60, 61]), these two processes stabilize the magnetism in V-doped AlN-zincblende. Similar magnetic behavior has been found for other group III nitride semiconductors such as BN, AlN, and InN in the zincblende structure doped with transition metals, for example Boukra et al. [62] and Espitia et al. [63] in their studies of the $\text{B}_{0.9375}\text{Mn}_{0.0625}\text{N}$ and $\text{B}_{0.9375}\text{V}_{0.0625}\text{N}$ compounds, respectively, while Doumi et al. [39] found the same behavior for $\text{Al}_{0.9375}\text{Mn}_{0.0625}\text{N}$ and $\text{In}_{0.9375}\text{Mn}_{0.0625}\text{N}$ and for $\text{Al}_{0.9375}\text{Fe}_{0.0625}\text{N}$ and $\text{In}_{0.9375}\text{Fe}_{0.0625}\text{N}$.

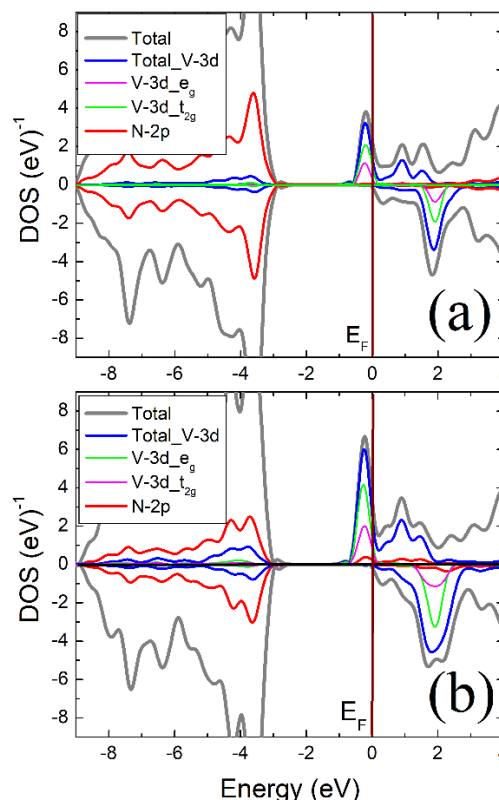


Figure 3. Total and partial DOS for (a) $\text{Al}_{0.0625}\text{V}_{0.9375}\text{N}$, (b) $\text{Al}_{0.125}\text{V}_{0.875}\text{N}$. Source: Authors.

As we can see in the DOS figure, the magnetic moment resides mainly on V atom, being the magnetic moment $2.0 \mu_B/\text{V-atom}$ in low stoichiometric. A similar result was obtained in a first-principles study of Mn-doped GaN in the zincblende structure

with a total magnetic moment of $2.0 \mu_B$. In this compound, the main contribution to the magnetic moment is attributed to the atom of Mn [39].

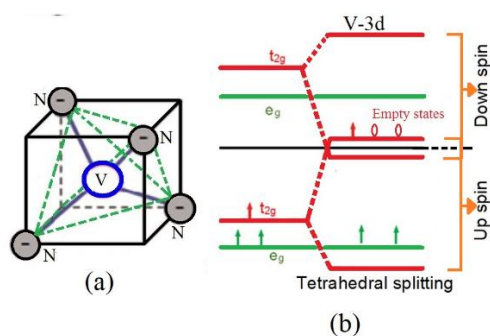


Figure 4. (a) V atom located in tetrahedral symmetry created by four N atoms, and (b) split between e_g and t_{2g} due to tetrahedral symmetry for both up-spin and down-spin. There is no contribution from the down-spin.

Source: Authors.

Finally, in order to verify the V-doped AlN-zincblende compound is a good candidate for possible application as diluted magnetic semiconductor material, we estimated the Curie temperature T_C using the classical Heisenberg model in the mean-field approximation, that is, $k_B T_C = 2\Delta E/x$ [48], where x is the number of V-atoms present in the AlN-zincblende, k_B is the Boltzmann constant, and ΔE is the difference in energy between the AFM and FM states. For the ground state of V-doped AlN in the zincblende structure, the T_C reaches ~ 410.8 °K, which is higher than room temperature. This indicates AlN-zincblende doped with V is a promising material to be a good diluted magnetic semiconductor and with potential applications as spin injector and other applications in spintronic.

CONCLUSIONS

In summary, we performed first-principles calculations of the structural, electronic, and magnetic properties of pristine AlN, $\text{Al}_{0.0625}\text{V}_{0.9375}\text{N}$, and $\text{Al}_{0.125}\text{V}_{0.875}\text{N}$ compounds in zincblende structure. Our studies predict a half-metallic behavior for $\text{Al}_{0.0625}\text{V}_{0.9375}\text{N}$, and $\text{Al}_{0.125}\text{V}_{0.875}\text{N}$ compounds, with the majority spin being metallic and the minority spin being semiconductor. These compounds possess magnetic properties with a calculated total magnetic moment of $2.0 \mu_B$ per V atom. The computational calculations predict a Curie temperature of 410.8 °K, which is higher than room temperature. Therefore, AlN doped with V is a promising candidate to be a good diluted magnetic semiconductor material.

ACKNOWLEDGEMENTS

The authors are very grateful to the Investigations center of the Universidad Distrital Francisco José de Caldas for its financial support

REFERENCES

- [1] S.C. Jain, M. Willander, J. Narayan, R. Van Overstrateten, J. Appl. Phys. 87 (2000) 965
- [2] I. Vurgaftman, J.R. Meyer, L.R. Ram-Mohan, J. Appl. Phys. 89 (2001) 5815.
- [3] I. Vurgaftman, J.R. Meyer, J. Appl. Phys. 94 (2003) 3675.
- [4] Schupp T, Lischka K., D. J. As, 2010 Journal of Crystal Growth 312 1500
- [5] Nakamura S, Senoh M, Iwasa N, Nagahama S, Yamada T and Makai T 1995 Japan. J. Appl. Phys. 34 L1332
- [6] Nakamura S 1997 The Blue Laser Diode GaN based Light Emitters and Lasers (Berlin: Springer)
- [7] Nakamura S 1999 Semicond. Sci. Technol. 14 R27
- [8] W.W. Lei, D. Liu, P.W. Zhu, X.H. Chen, Q. Zhao, G.H. Wen, Q.L. Cui, G.T. Zou, Applied Physics Letters 95 (2009) 162501.
- [9] Yao G, Fan G, Xing H, Zheng S, Ma J, Zhang Y and He L 2013 Journal of Magnetism and Magnetic Materials 331 117
- [10] Dinh V and Katayama-Yoshida H 2005 ferromagnetism and curie temperature of Vanadium-doped nitrides, Journal of Electron Microscopy 54 (Supplement 1) i61
- [11] Espitia M, Díaz J., Castillo L, International Journal of Physical Science 2016 11 11
- [12] Q.Y. Wu, Z.Q. Huang, R. Wu, L.J. Chen, Journal of Physics: Condensed Matter 19 (2007) 056209
- [13] R. Q. Wu, G. W. Peng, L. Liu, and Y. P. Feng, Z. G. Huang, Q. Y. Wu, Applied Physics Letters **89**, 142501 (2006)
- [14] Miguel J. Espitia R, John H. Díaz, César Ortega López, International Journal of Physical Sciences (10)17 (2015): 520-527.
- [15] Miguel J.Espitia R, Jonh H. Díaz, Luis Eduardo Castillo, International Journal of Physical Sciences (1)1 (2016) 11-18.
- [16] M.J. Espitia Rico, J. H. Díaz F, C. Ortega López, Journal of Physics: Conference Series 687 (2016) 012069
- [17] J.H. Díaz F, M.J. Espitia R, J.A. Rodríguez Martínez, Journal of Physics: Conference Series 743 (2016) 012004
- [18] R.M. Frazier, J. Stapleton, G.T. Thaler, C.R. Abernathy, S.J. Pearton, R. Rairigh, J. Kelly, A.F. Hebard, M.L. Nakarmi, K.B. Nam, J.Y. Lin, H.X. Jiang, J.M. Zavada, R.G. Wilson, J. Appl. Phys. 94 (2003) 1592.
- [19] S.Y. Wu, H.X. Liu, L. Gu, R.K. Singh, L. Budd, M. van Schilfgaarde, M.R. McCartney, D.J. Smith, N. Newman, Applied Physics Letters 82 (2003) 3047.
- [20] R.M. Frazier, J. Stapleton, G.T. Thaler, C.R. Abernathy, S.L. Pearton, R. Rairigh, J. Kelly, A.F. Hebard, M.L. Nakarmi, K.B. Nam, J.Y. Lin, H.X. Jiang, J.M. Zavada, R.G. Wilson, Journal of Applied Physics 94 (2003) 1592
- [21] D. Kumar, J. Antifakos, M.G. Blamire, Z.H. Barber, Appl. Phys. Lett. 84 (2004) 5004.

- [22] Wistrela E, Bittner A, Schneider M Reissner M and Schmid U 2017 *Journal of Applied Physics* 121 115302.
- [23] D. Pan, J. K. Jian, A. Ablat, J. Li, Y. F. Sun, and R. Wu, *J. Appl. Phys.* 112, 053911 (2012).
- [24] Y. Yang, Q. Zhao, X.Z. Zhang, Z.G. Liu, C.X. Zou, B. Shen, D.P. Yu, *Applied Physics Letters* 90 (2007) 092118
- [25] Pearton, *Appl. Phys. Lett.* 83, 1758 (2003).
- [26] K.Y. Ko, Z.H. Barber, M.G. Blamire, *J. Appl. Phys.* 100 (2006) 083905.
- [27] J. T. Luo, Y. Z. Li, X. Y. Kang, F. Zeng, F. Pan, P. Fan, Z. Jiang, and Y. Wang, *J. Alloys Compd.* 586, 469 (2014).
- [28] J. F. Murillo, C. Ortega, M. J. Espitia, *Journal of Physics: Conference Series* 687 (2016) 012114
- [29] Kai Li, Xiaobo Du, Yu Yan, Hongxia Wang, Qing Zhan, Hanmin Jin, *Physics Letters A* 374 (2010) 3671–3675
- [30] J.F. Murillo G, César Ortega López, Miguel J. Espitia R, *Results in Physics* 5 (2015) 281–285
- [31] I. Petrov, E. Mojab, R.C. Powell, J.E. Greene, *Appl. Phys. Lett.* 60 (1992) 2491
- [32] R. Thapa, B. Saha, K.K. Chattopadhyay, *Journal of Alloys and Compounds* 475 (2009) 373–377
- [33] Satoshi Mohri, Tsuyoshi Yoshitake, Takeshi Hara, Kunihito Nagayama, *Diamond & Related Materials* 17 (2008) 1796–1799
- [34] H. Ismail, E. Belloti, K.F. Brennan, J. Kolnik, R. Wang, P.P. Ruden, *J. Appl. Phys.* 81 (1997) 7827.
- [35] O. Ambacher, J. Majewski, C. Miskys, A. Link, M Hermann, M. Eickhoff, M. Stutzmann, F. Bernardini, V. Fiorentini, V. Tilak, B. Schaff, L.F. Eastman, *J. Phys.: Condens. Matter* 14 (2002) 3399.
- [36] C. Mietze, M. Landmann, E. Rauls, H. Machhadani, S. Sakr, M. Tchernycheva, F.H. Julien, W.G. Schmidt, K. Lischka, D.J. As, *Phys. Rev. B* 83 (2011) 195301.
- [37] D.J. As, *Microelectron. J.* 40 (2009) 204.
- [38] J. Simon, N.T. Pelekanos, C. Adelman, E. Martinez-Guerrero, R. André, B. Daudin, Le Si Dang, H. Mariette, *Phys. Rev. B* 68 (2003) 035312.
- [39] B. Doumi, A. Tadjer, F. Dahmane, D. Mesri, H. Aourag, *J. Supercond. Nov. Magn.* (2013) 26, 515–525
- [40] P. Giannozzi, S. Baroni, N. J. Bonin, a modular and open-source software project for quantum simulations of materials, *Condens. Matter*, 21 (2009) 395502.
- [41] Vanderbilt D, Soft self-consistent pseudopotentials in a generalized eigenvalue formalism, *Phys. Rev. B*, 41 (1990) 7892.
- [42] K. Laasonen, A. Pasquarello, R. Car, C. Lee, D. Vanderbilt, Car-Parrinello molecular dynamics with Vanderbilt ultrasoft pseudopotentials, *Phys Rev B*, 47 (1993) 10142.
- [43] Hohenberg, P., Kohn, W.: *Phys. Rev. B* 136, 864 (1964)
- [44] Kohn, W., Sham, L.J.: *Phys. Rev. A* 140, 1133 (1965)
- [45] J. Perdew, K. Burke, M. Ernzerhof, Generalized Gradient Approximation Made Simple, *Physical Review Letter*, 77 (1996) 3865.
- [46] H. Monkhorst, J. Pack, Special points for Brillouin-zone integrations, *Phys Rev B*, 13 (1976) 5188.
- [47] U.P. Verma, P.S. Bisht, *Solid State Sciences* 12 (2010) 665–669
- [48] A.E. Merad, M.B. Kanoun, J. Cibert, H. Aourag, G. Merad, *Materials Chemistry and Physics* 82 (2003) 471–477
- [49] S. Goumri-Said, M.B. Kanoun, A.E. Merad, G. Merad, H. Aourag, *Chem. Phys.* 302 (2004) 135
- [50] M.B. Kanoun, A.E. Merad, G. Merad, J. Cibert, H. Aourag, *Solid-State Electronics* 48 (2004) 1601–1606
- [51] C. Stampfl, C.G. Van de Walle, *Phys. Rev. B* 59 (1999) 5521.
- [52] Guangrui Yao, Guanghan Fan, Haiying Xing, Shuwen Zheng, Jiahong Ma, Yong Zhang, Longfei He, *Journal of Magnetism and Magnetic Materials* 331 (2013) 117–121
- [53] Zhao-Yong Jiao, Shu-Hong Ma, Ji-Fei Yang, *Solid State Sciences* 13 (2011) 331e336
- [54] N.E. Christensen, I. Gorczyca, *Phys. Rev. B* 50 (1994) 4397
- [55] P.E. van Camp, V.E. van Doren, J.T. Devreese, *Phys. Rev. B* 44 (1992) 9056; P.E. van Camp, V.E. van Doren, J.T. Devreese, *Solid State Commun.* 81 (1992) 23.
- [56] Y. Ohno, D.K. Young, B. Beschoten, F. Matsukura, H. Ohno, D.D. Awschalom, Electrical spin injection in a ferromagnetic semiconductor heterostructure, *Nature*, 402 (1999) 790
- [57] C. Vargas-Hernandez, M. Espitia-Rico M, R. Báez, Half-metallic ferromagnetism of $Zn_xMn_{1-x}O$ compounds: A first-principles study, *Computational Condensed Matter*, 4 (2015) 1–5.
- [58] Miguel J. Espitia R, Octavio Salcedo Parra, César Ortega López, *Journal of Magnetism and Magnetic Materials* 451 (2018) 295–299
- [59] X.Y. Cui, B. Delley, A.J. Freeman, C. Stampfl, *Phys. Rev. Lett.* 97 (2006) 016402
- [60] T. Dietl, H. Ohno, F. Matsukura, J. Cibert, D. Ferrand, *Science* 287 (2000) 1019.
- [61] T. Dietl, *Semicond. Sci. Technol.* 17 (2002) 377
- [62] A. Boukra A. Zaoui, M. Ferhat. Magnetic trends in $Ga_xMn_{1-x}N$, $Al_xMn_{1-x}N$, and $In_xMn_{1-x}N$ ternary systems: A first-principles study. *JOURNAL OF APPLIED PHYSICS* 108, 123904 2010
- [63] M.J. Espitia-Rico, J. Díaz, J.A. Martínez. Structural and electronic properties of V-doped cubic BN-A density functional theory study, *Solid State Communications*, 244 (2016) 23–27